Measuring Hubble's Constant in our Inhomogeneous Universe

XIANGDONG SHI[1], LAWRENCE M. WIDROW[2] and L. JONATHAN DURSI[3]

Department of Physics
Queen's University, Kingston, Ontario, K7L 3N6, CANADA

ABSTRACT

Recent observations of Cepheids in the Virgo cluster have bolstered the evidence that supports a Hubble constant in $70-90\,\mathrm{km\,sec^{-1}\,Mpc^{-1}}$ range. This evidence, by and large, probes the expansion of the Universe within 100 Mpc. We investigate the possibility that the expansion rate within this region is systematically higher than the true expansion rate due to the presence of a local, large underdense region or void. We begin by calculating the expected deviations between the locally measured Hubble constant and the true Hubble constant for a variety of models. The calculations are done using linear perturbation theory and are compared with results from N-body simulations wherever possible. We also discuss the expected correlations between these deviations and mass fluctuation for the sample volume. We find that the fluctuations are small for the standard cold dark matter as well as mixed dark matter models but can be substantial in a number of interesting and viable nonstandard scenarios. However, deviations in the Hubble flow for a region of radius 200 Mpc are small for virtually all reasonable models. Therefore, methods based on supernovae or the Sunyaev-Zel'dovich effect, which can probe 200 Mpc scales, will be essential in determining the true Hubble constant.

We discuss, in detail, the fluctuations induced in the cosmic background radiation by voids at the last scattering surface. In addition, we discuss the dipole and quadrupole fluctuations one would expect if the void enclosing us is aspherical or if we lie off-center.

[1]E-mail address: shi@astro.queensu.ca
[2]E-mail address: widrow@astro.queensu.ca
[3]E-mail address: dursi@astro.queensu.ca

1 Introduction

It is straightforward to measure the Hubble constant in a perfectly homogeneous and isotropic Universe: one simply divides the relative velocity between any two points by their separation. The situation is of course far more difficult in our inhomogeneous and anisotropic Universe. For most cosmologists, the working assumption is that the Universe becomes homogeneous on very large scales. The goal then is to find the recessional velocity and distance to an object sufficiently far away so that the Hubble flow dominates over peculiar velocities. In this work, we address the possibility that determinations of the Hubble constant have not yet reached such distances.

Knowledge of the true, global value of the Hubble constant, H_0, is central to any cosmological model. Most measurements to date place H_0 between $65 - 95\,\mathrm{km\,sec^{-1}\,Mpc^{-1}}$, values that are uncomfortably high given estimates of the age of the Universe based on globular cluster dating, and the theoretical prejudice that we live in a spatially flat, matter-dominated universe. In particular, if we accept that the Universe is older than 12 Gyr, then a Hubble constant $h > 0.55$ ($H_0 = 100\,h\,\mathrm{km\,sec^{-1}\,Mpc^{-1}}$) is incompatible with all $\Omega_\mathrm{m} = 1$ models (Ω_m is the density of matter in units of the critical density) and $h > 0.80$ is incompatible with all zero cosmological constant ($\Lambda = 0$) models. In addition, a high value for the Hubble constant is, in general, trouble for structure formation scenarios. This is especially true for cold dark matter (CDM) where the favoured value is $h \sim 0.3 - 0.4$. Finally, a low value for H_0 helps to close the gap between the prediction for the baryon density from big bang nucleosynthesis and recent determinations of the dark-to-baryonic matter ratio in rich clusters (Bartlett et al. 1994).

All resolutions to the "age problem" come at a cost. A true age for the Universe significantly less than 12 Gyr would require radical rethinking of stellar evolution (Cage & Walker 1992; Sandage 1993; Chaboyer 1994; Shi 1995). On the other hand, we can accommodate a universe older than 12 Gyr by requiring the Universe to be open, or by invoking a non-zero cosmological constant. For fixed h, an open Universe corresponds to an older one; but this is problematic especially if one accepts inflation which predicts $\Omega = 1$ in nearly all incarnations (see however Bucher et al. 1995, Linde 1995). Similarly, a universe dominated by a cosmological constant (or any energy density with negative pressure) will be older than the corresponding $\Omega_\mathrm{m} = 1$ universe. The cost here is the introduction of a new energy density term in the Friedmann equations whose origin is completely mysterious.

In many respects, a true Hubble constant of $50\,\mathrm{km\,sec^{-1}\,Mpc^{-1}}$ or less represents the simplest solution to the age problem. However, the majority of observations suggest that such values are ruled out. These include recent measurements by the Canada-France-Hawaii Telescope (CFHT) (Pierce et al. 1994) and the Hubble Space Telescope (HST) (Freedman et al. 1994) whose published values of $h = 0.87 \pm 0.07$ and $h = 0.80 \pm 0.17$, respectively, exclude a spatially flat, matter dominated

universe. Their Cepheid results are also consistent with other determinations based on techniques such as Tully-Fisher, planetary nebulae, and surface brightness fluctuations (see van den Bergh 1992 for a review). In principle, Cepheids should provide the most accurate method for determining the distance to Virgo. At present, there is the potential for large systematic errors (see, in particular, the paper by Freedman et al. 1994) due primarily to uncertainties in the position of the galaxy studied within Virgo. Measurements of Cepheids in other galaxies within the cluster will significantly reduce this uncertainty and provide a distance determination to Virgo of better than 10%.

Virgo is only 17 Mpc away, far too close for a reliable measurement of H_0. But it is only one additional rung of the distance ladder to clusters such as Coma which, at a distance ~ 100 Mpc, are assumed to be far enough away that their recessional velocities are dominated by the true Hubble flow.

But is this last assumption valid? Or is it possible that the local Hubble flow, as measured out to ~ 100 Mpc, overestimates the true Hubble constant by 20-30%? The discovery of large voids and sheet-like structures in redshift surveys (Kirshner et al. 1981; de Lapparent et al. 1986; Geller & Huchra 1989; da Costa 1991) and large scale bulk flows (Lauer & Postman 1994) on ~ 100 Mpc scales should give us pause as variations in the Hubble flow are likely to occur on comparable scales.

The question of deviations in the Hubble flow was addressed by Turner, Cen, and Ostriker (1992, hereafter TCO) in the context of a simple numerical experiment. A model universe (with a specified value for the global Hubble constant) is simulated using standard N-body methods and it is assumed that "observers" in this universe can accurately measure the distances to and radial velocities of *all* galaxies within a set distance R. Each observer constructs a Hubble diagram and reads off a value for the local Hubble constant $H_{\rm L}$. In this way, the effects of local deviations in the Hubble flow are separated out from observer-dependent effects such as systematic errors in distance determinations and incomplete sampling. The distribution of $H_{\rm L}$ measured by all observers in the simulation is studied and compared with other statistics of the density and velocity fields such as rms mass fluctuations and bulk flows. In the end, one can make probabilistic statements about the likelihood a given observer has for measuring a local Hubble constant within the range allowed by observations.

An alternate approach to this global statistical method is to explore specific and simple models for our local region of the Universe. Suppose, for example, we live in an underdense region or void. Any determination of the Hubble constant based on objects within this region will reflect the local expansion rate rather than the global one. The simplest model of this type has us at the center of a spherically symmetric section of an open spacetime embedded in a spatially flat Friedmann-Robertson-Walker universe (Suto et al. 1994; Wu et al. 1995; Moffatt & Tatarski 1994).

In Section 2 we take a second look at the statistical approach pioneered by TCO. Our interest is in studying a variety of models and so we use linear perturbation theory where probabilities can be

calculated directly from the linear power spectrum $P(k)$. Our first step is to compare linear theory results with those of TCO. As expected, agreement is good on large scales where perturbations are small. On small scales, linear theory tends to underestimate the rms fluctuations in $H_{\rm L}$. In addition, TCO find that the distribution of measured $H_{\rm L}$ has a distinctly non-Gaussian shape. We next use linear theory to study correlations between $H_{\rm L}$ and other observables. In particular, we derive the statistical relationship between $H_{\rm L}$ and the mass excess for the sample volume.

TCO consider the standard CDM scenario circa 1992 which is now known to be inconsistent with results from the COBE DMR experiment (Smoot et al. 1992) and the APM galaxy survey (Maddox et al. 1990). Here we use linear theory to calculate the rms fluctuations in $H_{\rm L}$ for a variety of observationally viable models. As one might expect, the size of deviations in the Hubble constant on 100 Mpc scales depends sensitively on the shape of the primordial power spectrum but is rather insensitive to the type of dark matter (i.e., hot, cold, or mixed) in the model.

Section 3 deals with the more direct approach of modeling our local region of the Universe. The simplest scenario is to assume that we are near the center of an underdense region that extends well past the Coma cluster. The mean density in this region must be fairly low ($\Omega_{\rm void} \lesssim 0.5$) in order that there be a significant difference between the true and measured values for the Hubble constant. This may not be so farfetched: there are hints from the number counts of galaxies that we live in a very large underdense region (Metcalfe et al. 1992) though interpretation of this data is complicated by evolutionary effects (see, for example, Loveday et al. 1992).

A large underdense region today implies rather significant perturbations in the energy density at the surface of last scattering. These perturbations lead to fluctuations in the cosmic background radiation (CBR) through the Sachs-Wolfe effect. We can therefore use CBR anisotropy measurements to limit the number of voids that reside in our Hubble volume. In addition, large angular-scale perturbations will be induced if our local underdense region is aspherical, or if we lie off-center. We can therefore place important constraints on this scenario by using the dipole and quadrupole anisotropy measurements.

Section 4 summarizes our results. Our general conclusion is that large fluctuations in $H_{\rm L}$ for $R \simeq 100$ Mpc can occur, but only in nonstandard models. For example, a CDM model with a tilted primordial power spectrum $P(k) \propto k^n; n > 1.5$ will have 2σ fluctuations in H in excess of 30%. However, even in these nonstandard models, fluctuations in H fall rapidly with increasing scale: Determinations of H based on objects ~ 200 Mpc away should reflect the global value to within 10% unless we live in an extremely rare, very large-scale underdense region.

There is, at present, considerable discrepancy among measurements for objects $\gtrsim 200$ Mpc away. The "expanding photosphere method" has been used to determine distances to 18 type II supernovae as far away as 180 Mpc (Schmidt et al. 1994) and references therein). An analysis of this data finds $h = 0.73 \pm 0.06({\rm statistical}) \pm 0.07({\rm systematic})\,{\rm km\,sec^{-1}\,Mpc^{-1}}$ with no evidence for

spatial deviations in the Hubble flow. In addition Lauer & Postman (1994) find that the value of H does not vary by more than 7% between 30 and $150h^{-1}$ Mpc. On the other hand, measurements for very distant ($R \gtrsim 400\,\mathrm{h}^{-1}$Mpc) objects based on the Sunyaev-Zel'dovich effect do seem to yield systematically lower values for h (Yamashita 1994; Birkinshaw & Hughes 1994) suggesting that we may in fact live in a low density, high h region of the Universe (Suto et al. 1994). The supernovae results and Lauer & Postman data seem to indicate that this void would be much larger than anything expected, even for fairly nonstandard models designed to give more power on large scales.

2 Hubble Constant Statistics

2.1 Linear Theory Analysis

In linear perturbation theory (Peebles 1993), the relationship between the peculiar velocity field and the density contrast $\delta(\mathbf{x}) \equiv (\rho(\mathbf{x}) - \rho_b)/\rho_b$ is given by

$$\mathbf{v}(\mathbf{x}) \;=\; \frac{2}{3H_0}\int d^3y\,\frac{\mathbf{x}-\mathbf{y}}{|\mathbf{x}-\mathbf{y}|^3}\,\delta(\mathbf{y}) \tag{1}$$

where $\rho(\mathbf{x})$, ρ_b and H_0 are the density field, background density, and global Hubble constant today. The peculiar Hubble flow, $\delta H(\mathbf{x}) \equiv H_L(\mathbf{x}) - H_0$ is

$$\delta H(\mathbf{x}) \;=\; \int d^3y\,\mathbf{v}(\mathbf{y})\cdot\frac{\mathbf{x}-\mathbf{y}}{|\mathbf{x}-\mathbf{y}|^2}W(\mathbf{x}-\mathbf{y}) \tag{2}$$

where $H_L(\mathbf{x})$ is the local value of the Hubble constant as measured by an observer at position $\mathbf{x}$ and $W(\mathbf{x}-\mathbf{y})$ is the window function for the observations. δH is essentially a breathing mode (expansion or contraction) of the peculiar velocity field, corresponding to the trace of the shear tensor (see, e.g. Kaiser 1988). For a perfectly volume limited sample out to a distance R, W is a step function, $W(\mathbf{x}-\mathbf{y}) = \theta(R - |\mathbf{x}-\mathbf{y}|)V_W^{-1}$ where $V_W \equiv 4\pi R^3/3$. In a Friedmann-Robertson-Walker universe, $\delta H \to 0$ for $R \to \infty$.

Equations (1) and (2) can be written in terms of the Fourier transform of the density contrast:

$$\frac{\delta H}{H_0} \;=\; \int \frac{d^3k}{(2\pi)^{3/2}}\,\delta(\mathbf{k})\,\mathcal{Z}(kR)\,e^{i\mathbf{k}\cdot\mathbf{x}} \tag{3}$$

where $\delta(\mathbf{k}) \equiv (2\pi)^{-3/2}\int d^3x\delta(\mathbf{x})e^{i\mathbf{k}\cdot\mathbf{x}}$,

$$\mathcal{Z}(x) \;=\; 3\,\frac{\sin(x) - \mathrm{Si}(x)}{x^3}\,, \tag{4}$$

and $\mathrm{Si}(x) \equiv \int_0^x dx\,\sin(x)/x$. The rms fluctuations in the local Hubble constant $\delta_H \equiv \langle(\delta H/H_0)^2\rangle^{1/2}$ ($\langle\ldots\rangle$ denotes spatial average) is given by

$$\delta_H^2 \;=\; \frac{1}{2\pi^2}\int k^2 dk P(k)\mathcal{Z}^2(kR) \tag{5}$$

where $P(k) = |\delta(\mathrm{k})|^2$ is the power spectrum. If the primordial perturbations are Gaussian, the distribution of δ_H will be Gaussian, at least in the linear regime.

R (Mpc)	δ_H (TCO)	δ_H (LT)	m (LT)	σ_{HM}
10	1.08	0.42	-0.64	1.07
20	0.45	0.23	-0.64	0.79
40	0.18	0.11	-0.65	0.55
60	0.10	0.071	-0.67	0.43
80	0.062	0.049	-0.67	0.35
120	0.029	0.027	-0.67	0.26

Table 1: TCO and Linear theory results for δ_H

2.2 TCO and Linear Theory

TCO use numerical simulations of cosmological models to generate a set of hypothetical observers. These observers can accurately measure the distances to and velocities of the galaxies within a pre-set distance. The local value of the Hubble constant, as measured by the kth observer, is given by

$$H_k \;=\; \frac{1}{N}\sum_{i\neq k}\frac{\mathbf{r}\cdot\mathbf{v_i}}{|\mathbf{r}|^2} \;+\; H_0 \tag{6}$$

where $\mathbf{r_i}$ and $\mathbf{v_i}$ are the position and velocity vectors of the ith galaxy, $\mathbf{r}\equiv\mathbf{r_i}-\mathbf{r_k}$, and the sum is over all N galaxies in the prescribed volume.

Eq (6) is essentially the discrete version of Eq (2) with the important distinction that Eq (2) involves a volume average whereas Eq (6) involves a sum over galaxies. Since galaxies tend to reside in high density regions (this will depend on biasing, i.e., galaxy formation) where the expansion rate is slower, the results of TCO will tend, on average, to be skewed towards negative values of $\delta H \equiv (H_k - H_0)/H_0$. This is indeed found to be the case.

Column 1 of Table 1 summarizes the results for δ_H from TCO. The results derived from linear theory for their model (baryon density, in units of the critical density, $\Omega_B = 0.05$; $h = 0.5$; $\Omega_{\rm m} + \Omega_B = 1$; rms mass fluctuation on $8h^{-1}\,$Mpc, $\sigma_8 = 0.67$) are shown in Column 2. As expected, the agreement is best on large scales where perturbations are small. On small scales, linear theory tends to underestimate δ_H. In any case, it is apparent that for this particular model, the local value of the Hubble constant, as measured by observers with complete coverage out to 100 Mpc, is expected to be with 5% or so of the true or global value.

2.3 Correlations between δ_H and other observables

A volume limited measurement of H cannot separate the peculiar Hubble flow within that volume from the true Hubble flow. There are, however, other quantities accessible to observers which characterize the peculiar velocity field and matter distribution. Correlations between such quantities

and the peculiar Hubble flow, if they exist, would provide a means for correcting our measurements of $H_{\rm L}$.

An obvious quantity to consider is mass fluctuation within the sample volume, $\delta M/M$. For an observer at the center of a spherically symmetric region with constant density contrast, $\delta H/H_0 = -\frac{1}{3}\delta M/M$ so long as $\delta \ll 1$. If this were the case, knowledge of $\delta M/M$ would be sufficient to correct local measurements of H. In general, however, there is only a statistical relationship between $\delta H/H_0$ and $\delta M/M$. TCO explore this relationship by plotting $\delta M/M$ versus $\delta H/H_0$ for the observers in their simulation (their Figure 6a). A linear fit is obtained by minimizing the total orthogonal distance of all points on this figure to the straight line

$$\frac{\delta H}{H_0} \;=\; m\frac{\delta M}{M} \;+\; b\,; \tag{7}$$

that is, by minimizing the function

$$\chi^2 \;=\; \frac{1}{1+m^2}\sum_i \left(\frac{\delta H_i}{H_0} - m\frac{\delta M_i}{M} - b\right)^2 . \tag{8}$$

Their result, $m = -0.60,\ b = -0.008$, corresponds to a slope that is nearly twice what one would naively expect from linear theory, and they attribute this difference to nonlinear effects. While they find substantial scatter in the plot, they conclude that δM offers the best hope for correcting local measurements of the Hubble constant.

Interestingly enough, the results of TCO are similar to those found in linear theory. Consider the linear theory expression for the fractional mass excess in a spherical top-hat region:

$$\frac{\delta M}{M} \;=\; \int \frac{d^3k}{(2\pi)^{3/2}}\,\delta(\mathbf{k})\,W(kR)\,e^{i\mathbf{k}\cdot\mathbf{x}} \tag{9}$$

where

$$W(x) \;=\; 3\,\frac{\sin(x) - x\cos(x)}{x^3}\ . \tag{10}$$

The rms mass fluctuation is given by

$$\delta_M^2 \;=\; \frac{1}{2\pi^2}\int k^2 dk P(k) W^2(kR). \tag{11}$$

In the limit $kR \to 0$, $\mathcal{Z} \to -1/3$ and $W \to 1$ which would seem to support the naive expectation. However, the window functions in Eq (5) and (11) differ not only in amplitude but in shape with $\mathcal{Z}$ having more support at larger k. A linear fit, analogous to the one calculated in TCO, yields

$$m = \frac{\delta_H^2 - \delta_M^2 + \sqrt{\left(\delta_H^2 - \delta_M^2\right)^2 + 4\left\langle \frac{\delta M}{M}\frac{\delta H}{H}\right\rangle^2}}{2\left\langle \frac{\delta M}{M}\frac{\delta H}{H}\right\rangle} \tag{12}$$

where

$$\left\langle \frac{\delta M}{M}\frac{\delta H}{H}\right\rangle \;=\; \frac{1}{2\pi^2}\int k^2 dk P(k)\mathcal{Z}(kR)W(kR) \tag{13}$$

The rms fluctuation from the best fit curve σ_{HM} is given by

$$\sigma_{HM}^2 = \frac{\delta_H^2 + m^2\delta_M^2 - 2m\left\langle \frac{\delta M}{M}\frac{\delta H}{H}\right\rangle}{(1+m^2)}. \tag{14}$$

Our results, shown in Table 1, illustrate that those of TCO can be largely explained by linear theory.

In principle, one can use knowledge of $\delta M/M$ in our region of the Universe to correct local measurements of H. With this in mind, we choose to determine the correlation between $\delta H/H_0$ and $\delta M/M$ by a slightly different procedure. Specifically, we fit minimize the distance of $\delta H/H_0$ to the curve given by Eq (7), i.e., we minimize

$$\chi^2 \;=\; \sum_i \left(\frac{\delta H_i}{H_0} - m\frac{\delta M_i}{M} - b\right)^2 . \tag{15}$$

A standard least squares analysis gives $m = \left\langle \frac{\delta M}{M}\frac{\delta H}{H}\right\rangle / \delta_M^2$ and $\sigma_{HM}^2 = \delta_H^2 - 2m\left\langle \frac{\delta M}{M}\frac{\delta H}{H}\right\rangle + m^2\delta_M^2$. We use these formulae to calculate m and σ_{HM} for the various models discussed above and give the results in Table 2.

2.4 Standard CDM and Variations

We calculate δ_H, m, and σ_{HM} for a variety of models specified by their power spectra $P(k)$. We begin by considering a family of models where the initial power spectrum is an $n = 1$, Harrison-Zel'dovich power law: $P_{\rm i}(k) = Ak$. The power spectrum today is given by P_i times an appropriate transfer function: $P(k) = AkT^2(k)$. Following Efstathiou, Bond, & White (1992) we choose the following parametric form for $T(k)$:

$$T(k) = \left(1 + \left(ak/\Gamma + (bk/\Gamma)^{3/2} + (ck/\Gamma)^2\right)^\nu\right)^{-1/\nu} \tag{16}$$

where $a = 6.4h^{-1}\,$Mpc, $b = 3.0h^{-1}\,$Mpc, $c = 1.7h^{-1}\,$Mpc, and $\nu = 1.13$. The power spectrum is therefore specified by Γ which determines the shape and A, or equivalently σ_8 which sets the normalization. $\delta_H \propto \sigma_8$ and so, in Figure 1, we show δ_H as a function of Γ/σ_8. The results are given for $h = 0.5$ and three different values of R. As expected, δ_H increases with decreasing Γ.

The Lauer & Postman (1994) velocity data on Abell clusters shows an large scale bulk motion that may indicate power on very large scales in excess of what is expected in most COBE normalized models. While there is still some controversy over the interpretation of this data (Strauss et al 1994, Feldman & Watkins 1994) it is useful to consider the implications these results would have for determinations of the Hubble constant, the idea being that a universe with large scale bulk flows might also have large breathing mode fluctuations in the peculiar velocity field that foil our attempts to measure H. Jaffe & Kaiser (1995) apply a likelihood analysis to the Lauer & Postman (1994) data using Eq (16), and find a peak in the likelihood function at $\sigma_8 \simeq 0.3$ and $\Gamma \simeq 0.025$.

From Figure 1, we see that this implies a rather modest δ_H: $\delta_H(R = 100\,\mathrm{Mpc}) = 0.05$. They note however, that there is a rather wide range of parameters that are consistent with the Lauer & Postman data. We see from their Figure 1, for example, that $\Gamma = 0.35$ and $\sigma_8 = 1.2$ is within the 68% confidence intervals for the COBE quadrupole measurement and also within the 50% likelihood contour for the Lauer & Postman data. For these parameters, $\delta_H \simeq 0.12$.

We next consider the following models: (1) Standard CDM (sCDM) with COBE normalization (Bunn, Scott, & White 1994): This is essentially the model considered in Section 2.2 but the $\sigma_8 = 1.38$. (2) Mixed dark matter (MDM): We use Holtzman's (1989) linear power spectrum for a 70% cold, 30% hot mixed dark matter model. Normalization is the same as in Model 1. (3) Tilted primordial $P(k)$ with spectral index $n > 1$. Models with both CDM and MDM are used. Again we normalize to the COBE results on large scales following Bunn, Scott, & White (1994). The results for these models are summarized in Table 2.

			Tilted CDM		MDM
	sCDM	MDM	n=1.15	n=1.5	n=1.5
δ_H(100 Mpc)	0.074	0.072	0.098	0.17	0.16
δ_H(150 Mpc)	0.040	0.041	0.052	0.083	0.083
δ_H(200 Mpc)	0.025	0.026	0.032	0.049	0.050
$(\delta H/H)$ vs. $(\delta M/M)$					
m(150 Mpc)	–0.60	–0.62	–0.60	–0.57	–0.59
σ(150 Mpc)	0.10	0.10	0.13	0.18	0.10

Table 2: Linear-theory $\delta_H(R)$, m, and σ for different power spectra $P(k)$.

Evidently, the rms peculiar Hubble flow on 100 Mpc scales can be quite substantial, especially for $n > 1$. These so-called blue primordial spectra (Lucchin et al. 1995) were introduced to boost power on 100 Mpc scales relative to COBE scales. Indeed, it is worth noting that the constraints on n from the COBE DMR experiment are not very restrictive, and $n = 1.5$ is easily allowed by the data (Bennett et al. 1994). A CDM model with $n > 1$ will no doubt lead to excessive power on small ($\lesssim 1$ Mpc) scales and this has motivated Lucchin et al. (1995) to consider $n > 1$ with MDM. Another potential difficulty with these models is that they can lead to large temperature fluctuations in degree-scale CBR experiments. Consider the usual decomposition of the CBR anisotropy: $\delta T/T(\theta,\phi) = \sum_{lm} a_{lm} Y_{lm}(\theta,\phi)$. For Gaussian perturbations, the temperature fluctuations are completely specified by the variance $C_l \equiv \langle |a_{lm}|^2 \rangle$. Following Kosowsky & Turner (1995) we estimate the effects of tilting the spectrum to be

$$C_l(n) \simeq \frac{l}{2}^{\ln(l/2)(n-1)} C_l(n=1) \tag{17}$$

For $l = 100$ we find that the temperature fluctuations ($\propto C_l^{1/2}$) are increased by a factor of 3 over the $n = 1$ model for $n = 1.15$ and 50 for $n = 1.5$. The latter case is clearly unacceptable unless degree-scale fluctuations are damped by a period of early reionization. In any case, the next generation of CBR experiments will lead to tighter constraints on the primordial spectrum and help settle this issue.

3 CBR Fluctuations from Voids

We have seen that the possibility of living in a large underdense region opens up the prospect for solving the H_0/t_0 problem without giving up spatial flatness or resorting to a cosmological constant (Suto et al. 1994; Wu et al. 1995; Moffatt & Tatarski 1994). In the simplest scenario, we would be at the center of an underdense region containing all of the objects used to measure H. We could then neglect safely the dynamics of the wall that separates this region from the rest of the Universe. For the CFHT and HST results this region would include the Coma cluster as well as clusters used to determine the peculiar velocity of Coma (as in, for example, Han & Mould (1992)). The region would therefore have to have a radius *significantly larger than* 100 Mpc. An even larger region would be required if one is to accommodate results from type II supernovae (e.g., Schmidt et al. (1994) which draw from objects up to 180 Mpc away. On the other hand, it may be possible to accommodate the CFHT and HST results with a local underdense region whose radius is *comparable to* 100 Mpc. This could arise if the Local Group and/or clusters such as Coma could lie on the surface of a void or perhaps on a ridge separating merging voids. Using N-body simulations to study interacting voids, Dubinski et al. (1993) find significant peculiar velocities tangential to the walls that separate merging voids, peculiar velocities that might help explain an anomalously high measurement of H. However, this scenario is inherently more complicated that the scenario in which the void contains the clusters used to determine H. In particular, the large scale peculiar velocity field is no longer characterized by a simple breathing mode.

The mean density in our region of the Universe must be fairly small if local measurements of H are to be significantly higher than the global value. In Figure 2 we show H_L, the expansion rate inside a uniform region, as a function of the density in that region, $\Omega_{\rm void}$. For $|\Omega_{\rm void} - 1| \ll 1$, we have the linear result discussed above: $H_L - H_0 = \frac{1}{3} H_0 (1 - \Omega_{\rm void})$. The HST and CFHT results with quoted error bars are also shown. We see that $t_0 > 12\,{\rm Gyr}$ and $H_{\rm L} > 63\,{\rm km\,sec^{-1}\,Mpc^{-1}}$ (the 1σ lower bound for the HST result) imply a local density $\Omega_{\rm void} \lesssim 0.55$, i.e., a nonlinear void.

Voids somewhat smaller than the ones required here appear to be quite common. Redshift surveys reveal a network of voids with typical diameters of $50 - 60$ Mpc (Kirshner et al. 1981; de Lapparent et al. 1986; Geller & Huchra 1989; da Costa 1991). There is also evidence for larger voids (Einasto, Joeveen, & Saar 1980, Bahcall & Soneira 1982) though, as one might expect, the larger voids are not nearly so empty. Of course, redshift surveys give the distribution of visible

galaxies and not the underlying matter distribution and so it is difficult to say what the true density contrast is inside the voids. Nevertheless, a picture emerges of a hierarchy of voids in which the density contrast decreases with increasing scale.

Galaxy counts and redshift surveys offer the possibility of directly probing the density and velocity fields in our region of the Universe. However, they are each plagued by a number of difficulties. In particular, evolutionary effects can mask or mimic density inhomogeneities in the galaxy counts. In addition, there is the question of how one normalizes this data. On the other hand, attempts to map the peculiar velocity field must contend with sparse sampling; the rich clusters used to probe the velocity field are just too rare.

Observations of anisotropies in the CBR present an alternative, and potentially clean probe of large scale density inhomogeneities. In this section we focus on constraints of large scale voids from CBR experiments. Previous attempts along these lines have used a statistical approach (Blumenthal et al. 1992; Piran et al. 1993). The idea was to construct a power spectrum that leads to a "reasonable number" of voids with the desired size and density contrast and to then see if this power spectrum is consistent with CBR observations. The discussion at the end of this section follows this approach. Here we focus on temperature fluctuations from individual voids and the primordial fluctuations that gave rise to them. In particular, we consider three distinct sources of temperature fluctuations: (1) primeval density fluctuations at the last scattering surface (primeval voids); (2) evolving voids between us and the last scattering surface (intermediate voids); and (3) the void enclosing us.

3.1 Formalism

Consider a spherically symmetric density perturbation in a matter dominated universe. The metric can be written (e.g., Kramer et al. 1980)

$$ds^2 = -dt^2 + e^{\lambda(\chi,t)}d\chi^2 + r^2(\chi,t)d\Omega^2 \ . \tag{18}$$

It is convenient to define the (spatially dependent) scale factor $a(\chi,t)$:

$$r(\chi,t) = a(\chi,t)\chi \ . \tag{19}$$

Let $a_i(\chi) = a(\chi,t_i)$ and $\rho_{\rm bi}$ be the scale factor and background density at some initial time t_i and let $\overline{\delta}(\chi)$ be the initial average density contrast enclosed by the $\chi = constant$ surface:

$$\overline{\delta}(\chi) = \overline{\rho}_i(\chi)/\rho_{\rm bi} - 1. \tag{20}$$

where $\overline{\rho}_i(\chi)$ is the average density contrast enclosed by the $\chi = constant$ surface. The equation of motion for $a(\chi,t)$ follows from the Einstein equations:

$$\frac{a(\chi,t)}{a_i(\chi)} \ = \ \frac{1+\overline{\delta}(\chi)}{2\overline{\delta}(\chi)}\frac{{\rm d}f(\eta)}{{\rm d}\eta}$$

$$H_i(\chi)[t + t_c(\chi)] \;=\; \frac{1+\overline{\delta}(\chi)}{2|\overline{\delta}(\chi)|^{3/2}}\frac{\overline{\delta}(\chi)}{|\overline{\delta}(\chi)|}f(\eta) \tag{21}$$

where $f(\eta) = \eta - \sin[\mathrm{h}]\eta$ for $\delta > [<]0$ and $H_i(\chi) = (\dot{a}/a)|_{t=t_i}$.

For a photon passing through the origin

$$\frac{\mathrm{d}\chi}{\mathrm{d}t} = \pm\frac{\sqrt{1-(4/9)\delta(\chi)\chi^2/t_i^2}}{r'}\,, \tag{22}$$

(Fang and Wu 1993) where the plus (minus) sign is for a photon moving away from (towards) the origin. The frequency shift of the photon is

$$\frac{\nu_i}{\nu_f} = \exp\left(\int_{t_i}^{t_f}\frac{1}{2}\dot{\lambda}dt\right) = \exp\left(\int_{t_i}^{t_f}\frac{\chi\dot{a}'+\dot{a}}{\chi a'+a}dt\right), \tag{23}$$

where ν_i is the frequency of the photon emitted at t_i and ν_f is the frequency of the photon observed at t_f. Here and throughout, we use overdot to denote partial derivative with respect to t and prime to denote partial derivative with respect to χ. The resultant temperature fluctuation for a blackbody distribution of photons passing through the center of the density fluctuation, in a spatially flat, matter-dominated universe, is

$$\frac{\delta T}{T} = \frac{\nu_f^{\mathrm{fluc.}} - \nu_f^{\mathrm{bkgd}}}{\nu_f^{\mathrm{bkgd}}} = \left(\frac{t_i}{t_f}\right)^{2/3}\exp\left(\int_{t_i}^{t_f}\frac{\chi\dot{a}'+\dot{a}}{\chi a'+a}dt\right) - 1\,. \tag{24}$$

By our convention, a negative $\delta T/T$ implies a cold spot in CBR sky.

The frequency shift of a photon passing through the center of a void is found by numerically integrating Eq (24). The calculation is straightforward when the density perturbation is linear but requires a special approximation, to be discussed in section 3.3, once the void becomes nonlinear. Spherical symmetry is assumed for the voids through out our calculation, unless explicitly stated otherwise.

3.2 Primeval Voids at the Last Scattering Surface

We assume that the voids present today result from the gravitational amplification of primordial perturbations. The alternative would be to have the voids produced after recombination by some non-gravitational process. The evolution of the spacetime inside a void is calculated from Eq (21). For definiteness, we assume a density profile of the form:

$$\overline{\delta}(\chi) = \left\{\begin{array}{cc} \delta_0, & \chi < \chi_1\cdot \\ -\delta_0\chi_1^3/(\chi_0^3-\chi_1^3), & \chi_1 \le \chi < \chi_0\cdot \\ 0, & \chi \ge \chi_0\cdot \end{array}\right\} \tag{25}$$

so that the ratio $\chi_1 : \chi_0$ determines whether one has a thick or thin wall. In Figure 3, we plot δ_0 as a function of Ω_{void} today. We see, for example, that $\Omega_{\mathrm{void}} \lesssim 0.55$ requires $\delta_0 \lesssim -8.5\times10^{-4}$ at recombination.

The correspondence between the size of the primeval void and its size today is trickier. In the linear regime, the size of the void can be easily calculated from Eq (21). In the nonlinear regime, matter from both inside and outside the void piles up on its surface (Maeda & Sato 1983a; Berschinger 1985). In any case, the size of the void can grow no faster than the expansion rate inside the void: A void that has $\Omega_{\rm void} = 0.55$ today grew no more than 20% (in comoving coordinates) from the time of recombination.

Density perturbations at the time of recombination lead to temperature fluctuations in the CBR sky. If the scale of the perturbation l is much larger than the horizon size at recombination, $ct_{\rm rec}$, the temperature fluctuations will be dominated by the Sachs-Wolfe effect (Sachs & Wolfe 1968). The expected temperature fluctuation is

$$\frac{\delta T}{T} \sim -\frac{\delta\rho}{\rho}\left(\frac{l}{ct_{\rm rec}}\right)^2. \tag{26}$$

where we have omitted a prefactor of order 0.1. For $l \lesssim ct_{\rm rec}$, other effects such as the Doppler peak and adiabatic fluctuations in baryons become important (Hu, Sugiyama, & Silk 1995).

Figure 4 shows our numerical calculation of the Sachs-Wolfe effect for a primeval void with $\delta_0 = -8.5 \times 10^{-4}$ and $\chi_1 = 67h^{-1}/(1+z_{\rm rec})$ Mpc and three different density profiles. $\chi_{\rm LSS}$ is the distance from the last scattering surface to the center of the void with negative values corresponding to the situation in which the last scattering surface lies behind the center of the void. In these calculations, we neglect the thickness of the last scattering surface since it is unimportant so long as $\chi_1 \gg 10h^{-1}/(1+z_{\rm rec})$ Mpc. Note that the temperature fluctuations scale linearly with δ_0.

We see that sign and magnitude of the temperature fluctuation depends sensitively on where the last scattering surface intercepts the void. In addition, while the maximum temperature fluctuation is relatively insensitive to the thickness of the wall, the range in values of $\chi_{\rm LSS}$ over which $\delta T/T$ is large increases as we increase the thickness of the wall.

We wish to calculate the number of CBR fluctuations as a function of angular diameter and amplitude. Let $n_{\rm void}^{\rm rec}$ be the number density of voids that lead to CBR fluctuations with the desired amplitude and angular size. The expected number of fluctuations seen by a given experiment will be

$$\begin{aligned}\langle\mathcal{N}\rangle &\simeq 4\pi\left(\frac{3ct_0}{1+z_{\rm rec}}\right)^2 n_{\rm void}^{\rm rec}\chi_1\mathcal{P} \\ &\approx 14h^{-3}\ {\rm Mpc}^3\cdot n_{\rm void}^{\rm rec}\left[\frac{\chi_1}{100\,{\rm Mpc}/(1+z_{\rm rec})}\right]\mathcal{P}\end{aligned} \tag{27}$$

The COBE DMR experiment has mapped the entire sky with 7° resolution. Primeval voids with $\chi_1 \gtrsim 350h^{-1}/(1+z_{\rm rec})$ and $\delta_0 \lesssim -8.5\times10^{-4}$ lead to fluctuations that would have been easily seen in this experiment. We therefore require $\langle\mathcal{N}\rangle \lesssim 1$ for these very large voids. This implies a tight constraint on their number density today, $n_{\rm void}^0 = n_{\rm void}^{\rm rec}/(1+z_{\rm rec})^3$:

$$n_{\rm void}^0 \lesssim 2\times10^{-11}h^3\left[\frac{100/(1+z_{\rm rec}){\rm Mpc}}{\chi_1}\right]\ {\rm Mpc}^{-3}$$

$$\lesssim \quad 5 \times 10^{-11} \ \mathrm{Mpc}^{-3}. \tag{28}$$

Degree-scale measurements of temperature fluctuations in the CBR place constraints on smaller-scale voids. The MAX and MSAM experiments cover ~ 40 square degrees in total ($\mathcal{P} \simeq 0.001$) with 0.5° resolution and find an rms temperature fluctuation of $|\delta T/T| \lesssim 6 \times 10^{-5}$ (Meinhold and Lubin 1991; Alsop et al. 1992; Meinhold et al. 1993; Gundersen et al. 1993; Devlin et al. 1994; Clapp et al. 1994; Cheng et al. 1994). Figure 5 shows the absolute value of $\delta T/T$ in the direction of the center of the void, averaged over $-0.5 < \chi_{\rm LSS}/\chi_0 < 0.5$. From Figure 5, we see that primeval voids with $\delta_0 \leq -8.5 \times 10^{-4}$, $\chi_1 \gtrsim 50h^{-1}(1+z_{\rm rec})^{-1}$ Mpc, and $\chi_0 : \chi_1 = 3:1$ (thick wall case) or $\chi_1 \gtrsim 80h^{-1}(1+z_{\rm rec})^{-1}$ Mpc and $\chi_0 : \chi_1 = 9:8$ (thin wall case) can easily lead to temperature fluctuations that exceed the observational limit. Several individual patches with $|\delta T/T|$ as large as 1×10^{-4} have been observed though it is not as yet clear if these rare large fluctuations represent true CBR anisotropies or foreground contamination. In any case, primeval voids with $\delta_0 \leq -8.5 \times 10^{-4}$ and $\chi_1 \gtrsim 50h^{-1}(1+z_{\rm rec})^{-1}$ Mpc (thick wall) or $\chi_1 \gtrsim 80h^{-1}(1+z_{\rm rec})^{-1}$ Mpc (thin wall) should be rare in the currently covered area of MAX and MSAM. To be conservative, we require $\langle \mathcal{N} \rangle < 10$. This yields the constraints

$$n^0_{\rm void} \lesssim 3 \times 10^{-7} h^3 \mathrm{Mpc}^{-3}. \tag{29}$$

This implies that $\lesssim \mathcal{O}(0.1)$ of the volume of our universe can be occupied by these voids.

3.3 Voids at Intermediate Redshift

Temperature fluctuations due to nonlinear structures between us and the last scattering surface were first considered by Rees and Sciama (1968). For subhorizon-sized structures, the temperature fluctuation will be $\mathcal{O}((R/ct)^3)$ where R is the physical size of the object at the time t when the photon crosses it.

We use the formalism of Section 3.1 to calculate temperature fluctuations due to an intermediate nonlinear void of arbitrary interior density. For simplicity, we assume the a thin wall separates the void from the rest of the Universe. For the special case of a vacuum void, Thompson and Vishniac (1987), and Martínez-González et al. (1990), find

$$\frac{\delta T}{T} \approx \left(\frac{R}{ct}\right)^3 \cos\Psi \left(\frac{8}{9}\gamma - \frac{16}{27} - \frac{16}{81}\cos^2\Psi\right) \tag{30}$$

where Ψ is the angle between the photon's direction and a line from the center of the void to the exit point of the photon. γ describes the expansion of the void: $R \propto t^\gamma$.

The numerical integration of Eq (24) must be modified in order to handle the nonlinear voids considered here. In the formalism outlined above, the initial density perturbation is divided into concentric, spherical shells. However, once the density fluctuation becomes nonlinear and matter starts to pile up on the wall of the void, shell-crossing will occur. To avoid complications due

to shell-crossing, we choose instead to divide the density profile into concentric shells at the time when the photons exit the void. The "evolution" of the void is now found by solving the same equations as before, but letting time run backwards. However now, there is no shell crossing and the frequency shift of the photons can be calculated using the same methods as in section 3.1.

The expansion rate inside the void is still calculated by evolving the initial perturbation (i.e., the perturbation at recombination) forward in time. This calculation not only determines H_L but also the velocity perturbation associated with the void at the time when the photons exit the void. The latter is required for our backward-time integration. The index γ for the expansion of the wall is put in by hand. In general, $0.667 \leq \gamma \leq 0.8$. $\gamma = 2/3$ corresponds to the case where the wall expands with the background, a situation that will arise when the wall collides with the walls enclosing neighboring voids. $\gamma = 0.8$ corresponds to a single isolated void. The result is easily derived from either energy or momentum conservation (Maeda and Sato 1983a; Berschinger 1985).

For a nearby vacuum void with a thin wall and a radius of $100h^{-1}$ Mpc, eq. (30) yields approximately -1×10^{-5} for $\gamma = 0.8$, and -2.5×10^{-5} for $\gamma = 2/3$ in the direction of the center of the void. Our calculations yield -7×10^{-6} and -2.6×10^{-5} respectively. Our calculations also confirmed the scaling law of $\delta T/T \propto (R/ct)^3$. Empirical comparisons indicate that our results are reliable to order $\mathcal{O}(10^{-6})$.

Figure 6 shows our results for a void with a $100h^{-1}$ Mpc radius and with different $\Omega_{\rm void}$ under a thin wall approximation. $\delta T/T$ is the CBR temperature fluctuation in the direction through the center of the void. It is assumed that we are located just outside the wall. The figure indicates that the $\delta T/T$ due to a nearby $100h^{-1}$ Mpc void is not large enough to be constrained by COBE measurements. However, according to the $(R/ct)^3$ scaling law, voids with a radius $\gtrsim 200h^{-1}$ Mpc (thus yielding $\gtrsim 8$ times more temperature fluctuation) and a sufficiently low $\Omega_{\rm void}$ can be in conflict with the COBE observation.

3.4 The Void Enclosing Us

For spherical voids between us and the last scattering surface, the leading order ($\mathcal{O}(R/ct_0)$) and the second order ($\mathcal{O}(R/ct_0)^2$) contributions to the CBR anisotropy cancel (Rees & Sciama 1968). For the void enclosing us, this cancellation does not occur and we have a contribution to the dipole component of the CBR of $\mathcal{O}(R/ct_0)$. This contribution can be viewed simply as arising from our peculiar motion relative to the CBR rest frame and its amplitude is easy to estimate:

$$\left|\frac{\delta T}{T}\right|_{\rm dipole} = \left(H_{\rm void}t_0 - \frac{2}{3}\right)\frac{r}{ct_0}, \tag{31}$$

Here r is the our distance to the center of the void, as illustrated in the geometry of Figure 7. A detailed calculation, making use of the formalism developed above, leads to similar results. In Figure 8, we show the amplitude of the dipole moment as a function of r for $0 \leq \Omega_{\rm void} \leq 0.55$.

The requirement that $|\delta T/T| \lesssim 10^{-3}$ leads to the constraints $r \lesssim 7\,\mathrm{h}^{-1}$Mpc for a vacuum void, and $r \lesssim 22\,\mathrm{h}^{-1}$Mpc for $\Omega_{\rm void} = 0.55$.

The contribution to higher order moments from the void enclosing us is $\mathcal{O}((R/ct_0)^3)$ and can lead to unacceptably large fluctuations for $R \gtrsim 200h^{-1}$ Mpc, unless we are essentially at the center.

Thus far we have assumed perfect spherical symmetry for the voids. This is no doubt unrealistic, though it does appear that voids become more spherical with time (Blaes et al. 1990). Clearly, deviations from spherical symmetry will lead to CBR distortions. Consider, for example, a bump in the wall with height ΔR (Figure 7). We estimate of its order of magnitude as follows. The deviation from spherical symmetry should contribute to temperature fluctuation at orders $(R/ct_0)^m(\Delta R/R)^n$, where m and n are positive integers. The leading order, with $m = n = 1$, is simply a dipole resembling eq. (31). The next order terms, with $m + n = 3$, contribute to higher order moments. (For spherical symmetry (Rees and Sciama 1968), only the $m = 3$, $n = 0$ term is relevant.) By requiring contributions at these orders to be smaller than 10^{-5}, the level of anisotropy measured by COBE at $\gtrsim 10^\circ$ angular scale, we can constrain the size of the deviation ΔR. For $R \lesssim 100h^{-1}$ Mpc, a bound is estimated by considering the $m = 1$, $n = 2$ term:

$$\left|\frac{\delta T}{T}\right| \sim (\Delta H)t_0 \left(\frac{R}{ct_0}\right)\left(\frac{\Delta R}{R}\right)^2 \lesssim 10^{-5}, \tag{32}$$

where ΔH is the difference between the expansion rates inside and outside the void, which is roughly $H_0(1 - \Omega_{\rm void})/3$ in linear theory. Eq. (32) amounts to

$$\frac{\Delta R}{R} \lesssim 0.03\sqrt{\frac{100h^{-1}\mathrm{Mpc}}{R(1 - \Omega_{\rm void})}} \tag{33}$$

at $\gtrsim 10^\circ$ angular scale. If $R \gtrsim 100h^{-1}$ Mpc, a bound, estimated from the $m = 2$, $n = 1$ term, gives

$$\frac{\Delta R}{R} \lesssim \frac{0.02}{1 - \Omega_{\rm void}}\left(\frac{100h^{-1}\mathrm{Mpc}}{R}\right)^2 . \tag{34}$$

Therefore, a $200h^{-1}$ Mpc radius void must be spherically symmetric to $\sim 1\%$ to avoid a contradiction with the COBE results.

4 Discussion and Conclusions

The Hubble constant sets both the distance and time scales for the Universe and therefore plays a central role in all cosmological models. Numerous observations place its value between 65 and $95\,\mathrm{km\,sec^{-1}\,Mpc^{-1}}$. If indeed the true value is in this range, and if the Universe is as old as the globular cluster experts say it is, then fairly radical modifications to the standard $\Omega_{\rm m} = 1$ paradigm will be called for.

In this paper, we explore the possibility that the true Hubble constant $H_0 \simeq 50\,\mathrm{km\,sec^{-1}\,Mpc^{-1}}$, not because of systematic errors in current observations, but because these observations do not reach deep enough into the cosmos.

Possible discrepancies between the locally measured value for H and the true value are quantified in $\delta_H = \delta_H(R)$ where R is the radius of the sample volume. We outline a simple procedure for calculating δ_H based on linear perturbation theory. Where applicable, we compare the results with those based on the N-body simulations of TCO. Our conclusions are as follows:

• Linear and nonlinear theories are in good agreement on large scales.

• For $R \gtrsim 100\,\mathrm{Mpc}$, δ_H is insensitive to the type of dark matter present in the model.

• δ_H is correlated with the mass fluctuation within the sample. In particular, a measurement of $\delta M/M$ leads to the prediction $\delta H/H_0 = -(0.6 \pm 0.15)\delta M/M$.

• $\delta_H(R = 100\,\mathrm{Mpc}) \simeq 0.07$ for standard $n = 1$ CDM as well as $n = 1$ MDM. If these models describe our Universe, then the HST and CFHT results, in all likelihood, reflect the true value.

• $\delta_H(R = 100)\,\mathrm{Mpc} > 0.1$ for nonstandard models with extra power on large scales. These include an $n = 1$ CDM-like model with $\Gamma = 0.35$ and $\sigma_8 = 1.2$ (see Eq (16)) and either CDM or MDM with a tilted, $n = 1.5$ primordial spectrum. If our Universe is described by either of these models, then measurements of H will have to reach $\sim 200\,\mathrm{Mpc}$ where δ_H drops well below 0.1.

Galaxy counts and redshift surveys allow us the opportunity to directly probe the density and velocity field in our region of the Universe. Unfortunately, the interpretation of these observations is not so straightforward. In the case of the galaxy counts, for example, it is difficult to separate density inhomogeneities from evolutionary effects. On the other hand, analysis of the velocity data is made difficult by sparse sampling. CBR anisotropy measurements offer an alternative, and potentially clean probe of the large scale inhomogeneities discussed in this paper. Here, we calculate the expected temperature fluctuations due to voids at the last scattering surface; between us and the last scattering surface; and by the void enclosing us. The results are compared with existing data from the COBE DMR experiment, and by degree-scale experiments such as MAX and MSAM. A summary of our conclusions follows:

• No more than a handful of voids with radii $\gtrsim 400\,\mathrm{h^{-1}Mpc}$ can exist in our Hubble volume.

• Smaller voids are constrained by degree-scale CBR experiments. We find that the number density today of voids with radii $\gtrsim 60\,\mathrm{h^{-1}Mpc}$ and $\Omega_{\mathrm{void}} \leq 0.55$, under the current sky coverage of degree-scale CBR experiments, is $\lesssim 3 \times 10^{-7} h^3\,\mathrm{Mpc}^{-3}$, occupying $\mathcal{O}(0.1)$ of our Hubble volume.

• If the void enclosing us has a radius $\gtrsim 200\,\mathrm{h^{-1}Mpc}$, large dipole and quadrupole anisotropies will be induced, unless, of course, the void is very nearly spherical, and we are near the center.

5 Acknowledgments

We thank Andrew Jaffe, Kyle Lake, Man Hoi Lee, Sharon Vadas, and Rick Watkins for helpful discussions. This work is supported by the Natural Science and Engineering Research Council of Canada. X. Shi is supported, in part, by the Canadian Institute for Theoretical Astrophysics through the CITA National Fellow program.

References

Alsop, D. C. et al. 1992, ApJ, 395, 317

Bartlett, J. G. et al. 1994, Nature, submitted; astro-ph/9407061

Bennett, C. L. et al., 1994, COBE preprint #94-01; astro-ph/9401012

Berschinger, E. 1985, ApJS, 58, 1

Birkinshaw, M. & Hughes, J. P., 1994, ApJ, 420, 33

Blaes, O. M., Glodreich, P., & Villumsen, J. V. 1990, ApJ, 361, 331

Blumenthal, G. R., da Costa, L. N., Goldwirth, D. S., Lecar, M. & Piran, T. 1992, ApJ, 388, 234

Broadhurst, T. J. et al. 1990, Nature, 343, 726

Bucher, M., Glodhaber, A. S., & Turok, N., 1995, hep-ph/9501396

Bunn, E. F., Scott, D. & White, S. D. M., 1994, astro-ph/9409003

Chaboyer, B. 1994, ApJL, submitted; CITA 94-52

Cheng, E. S. et al. 1994, ApJL, 422, L37

Clapp, A. C. et al. 1994, ApJL, 433, L57

de Lapperent, V., Geller, M. J. & Huchra, J. P., 1986, ApJL, 302, L1

Devlin, M. J. et al. 1994, ApJL, 430, L1

Dodelson, S. & Stebbins, A. 1994, ApJ, 433, 440

Dubinski, J., et al., 1993, ApJ, 410, 458

Efsthathio, G., Bond, J.R. & White S. D. M., 1992, MNRAS, 258, 1p

Fang, L., & Wu, X. 1993, ApJ, 408, 25

Feldman, H. A., & Watkins, R. 1994, ApJ, 430, L17

Freedman W. et al. 1994, Nature, 371, 757

Geller, M. J. & Huechra, J. P., 1989, Science, 246, 897

Gundersen, J. O. et al. 1993, ApJL, 413, L1

Han, M. & Mould, J. R., 1992, ApJ, 396, 453

Holtzman, J., 1989, ApJSS, 71, 1

Hu, W., Sugiyama, N., & Silk, J. 1995, Nature, submitted; astro-ph/9504057.

Jaffe, A. H. & Kaiser, N., 1994, ApJL, submitted; astro-ph/9408046

Kaiser, N., 1988, Mon. Not. R. A. S., 231, 149

Kirshner, R. P., Oemeler, A., Schecter, P. L. & Shectman, S. A., 1981 ApJL, 248, L57

Kramer, D. et al. 1980, *Exact Solutions of Einstein's Field Equations*, Chapter 13, and references therein (Cambridge University Press).

Lauer, T. R. & Postman, M., 1994, ApJ, 425, 418

Linde, A. 1995, Phys. Lett. B, 351, 99

Loveday, J., Peterson, B. A., Efstathiou, G., & Maddox, S. J. 1992, ApJ 390, 338

Lucchin et al., 1995, ApJ, submitted; astro-ph/9504028

Maddox, S. J., Efstathiou, G., Sutherland, W. J. & Loveday, J. 1990, MNRAS, 242, 43p

Maeda, K., & Sato, H. 1983a, Prog. Theor. Phys., 70, 772

Maeda, K., & Sato, H. 1983b, *ibid.*, 1276

Martínez-González, E., Sanz, J. L., & Silk, J. 1990, ApJL, 355, L5

Meinhold, P., & Lubin, P. 1991, ApJL, 370, L11

Meinhold, P. et al., 1993, ApJL, 409, L1

Metcalfe, N., Shanks, T., Roche, N., & Fong, R. 1993, Ann. of the NY Acad. of Sci., 688, 534

Moffat, J. W., & Tatarski, D. C. 1994, UTPT-94-19; astro-ph/9407036

Nicolaci da Costa, L. et al., 1991, ApJSS, 75, 935

Peebles, P. J. E. 1993, *Principles of Physical Cosmology* (Princeton University Press, Princeton, New Jersey)

Pierce, M. et al. 1994, Nature, 371, 385

Piran, T., Lecar, M., Goldwirth, D. S., da Costa, L. N., & Blumenthal, G. R. 1993, MNRAS, 265, 681

Rees, M. J., & Sciama, D. W. 1968, Nature, 217, 511

Sachs, R. K., & Wolfe, A. M. 1968, ApJ, 147, 73

Sandage, A. 1993, AJ, 106, 719

Schmidt, B. P. et al. 1994, ApJ, 432, 42

Shi, X. 1995, ApJ, in press

Smoot, G. et al. 1992, ApJL, 396, L1

Strauss, M. A., et al., 1994 preprint

Suto, Y., Suginohara, T., & Inagaki, Y. 1994, Prog. Theor. Phys., submitted; astro-ph/9412090

Thompson, K. L., & Vishniac, E. T. 1987, ApJ, 313, 517

Turner, E. L., Cen, R., & Ostriker, J. P., 1992, AJ, 103, 1427 (TCO)

van den Bergh, S., 1992, Publ. Astron. Soc. Pac., 104, 861

Wu, X. et al. 1995, ApJL, submitted; astro-ph/9512082

Yamashita, K. 1994 in New Horizon of X-Ray Astronomy, ed. F. Makino & T. Ohashi (Universal Academy Press, Tokyo), 279

Figure Captions:

Figure 1. δ_H, the rms deviation in the Hubble flow, as a function of the transfer function parameterized by Γ (Eq (16)) for scales $R = 100,\ 150,$ and $200\,\mathrm{Mpc}$, $h = 0.5$, $\Omega_\mathrm{m} = 1$, and $\sigma_8 = 1$. δ_H scales linearly with σ_8.

Figure 2. The relation between H_L, Ω_void, and t_0 in an $\Omega_\mathrm{m} = 1$, $\Lambda = 0$ universe.

Figure 3. The relation between the initial density fluctuation δ_0 in a primeval void and the density parameter Ω_void it would have today.

Figure 4. The temperature fluctuation of CBR in the direction of the center of a primeval void, due to the Sachs-Wolfe effect, vs. the position of the last scattering surface relative to the center of the void. The initial density fluctuation is assumed to be $\delta_0 = -8.5 \times 10^{-4}$. Different lines stands for cases with different wall thickness.

Figure 5. The averaged temperature fluctuation magnitude in CBR from a primeval void, vs. the coordinate radius of the void, for three different wall thickness. The dot-dash line shows the temperature fluctuation vs. the coordinate radius of the void when the last scattering surface cut through the center of the void. The initial density fluctuation is assumed to be $\delta_0 = -8.5 \times 10^{-4}$.

Figure 6. The temperature fluctuation magnitude in CBR from a intermediate void with a radius of $100h^{-1}$ Mpc, vs. the density parameter Ω_void inside the void. We are assumed to be just outside the void. The solid line: $\gamma = 2/3$; the dash line: γ as calculated from momentum conservation of the wall.

Figure 7. The geometry of a void enclosing us. The dashed line illustrate a deviation of the wall of the void from a perfect sphere. ΔR is the height of the deviation.

Figure 8. The amplitude of a CBR dipole moment $|\delta T/T|_\mathrm{dipole}$ contributed by a void enclosing us vs. the distance between us and the center of the void r. No peculiar velocity other than that due to the faster expansion inside the void is assumed for us.

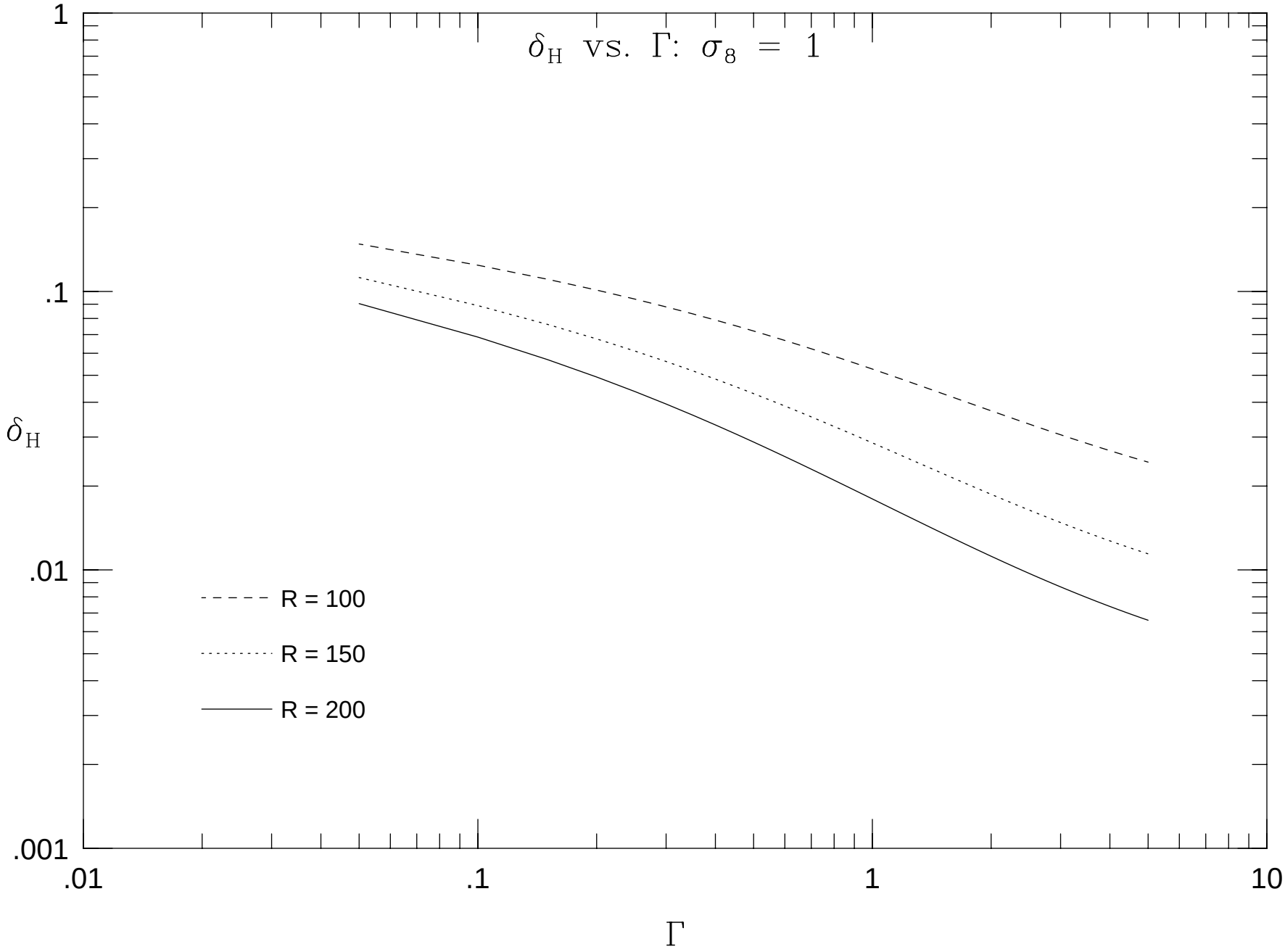
δ_H vs. Γ: $\sigma_8 = 1$
1
.1
.01
.001
δ_H
.01
.1
1
10
Γ
R = 100
R = 150
R = 200

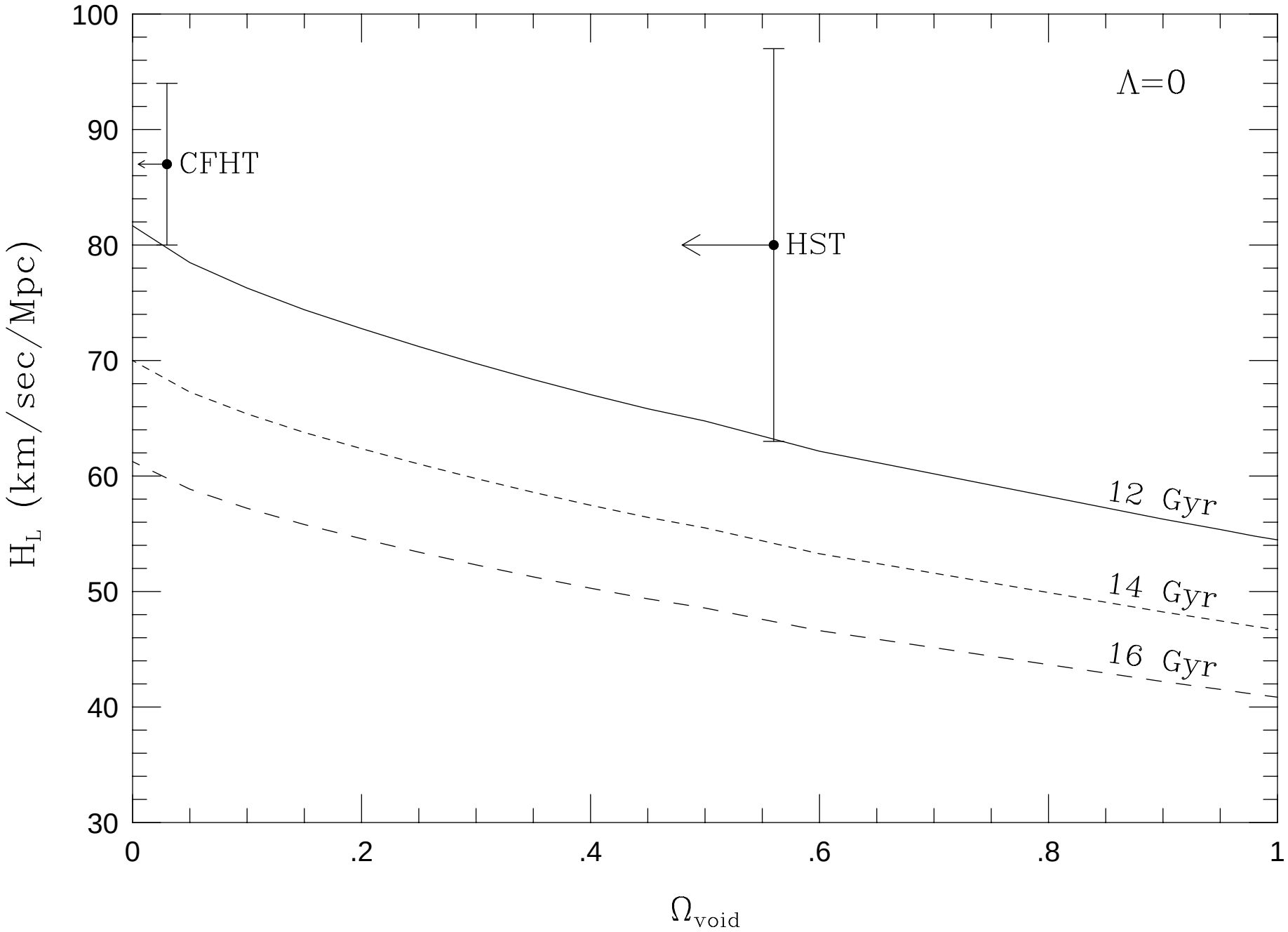
100
90
80
70
60
50
40
30
0
.2
.4
.6
.8
1
H_L (km/sec/Mpc)
Ω_{void}
Λ=0
CFHT
HST
12 Gyr
14 Gyr
16 Gyr

Figure 2

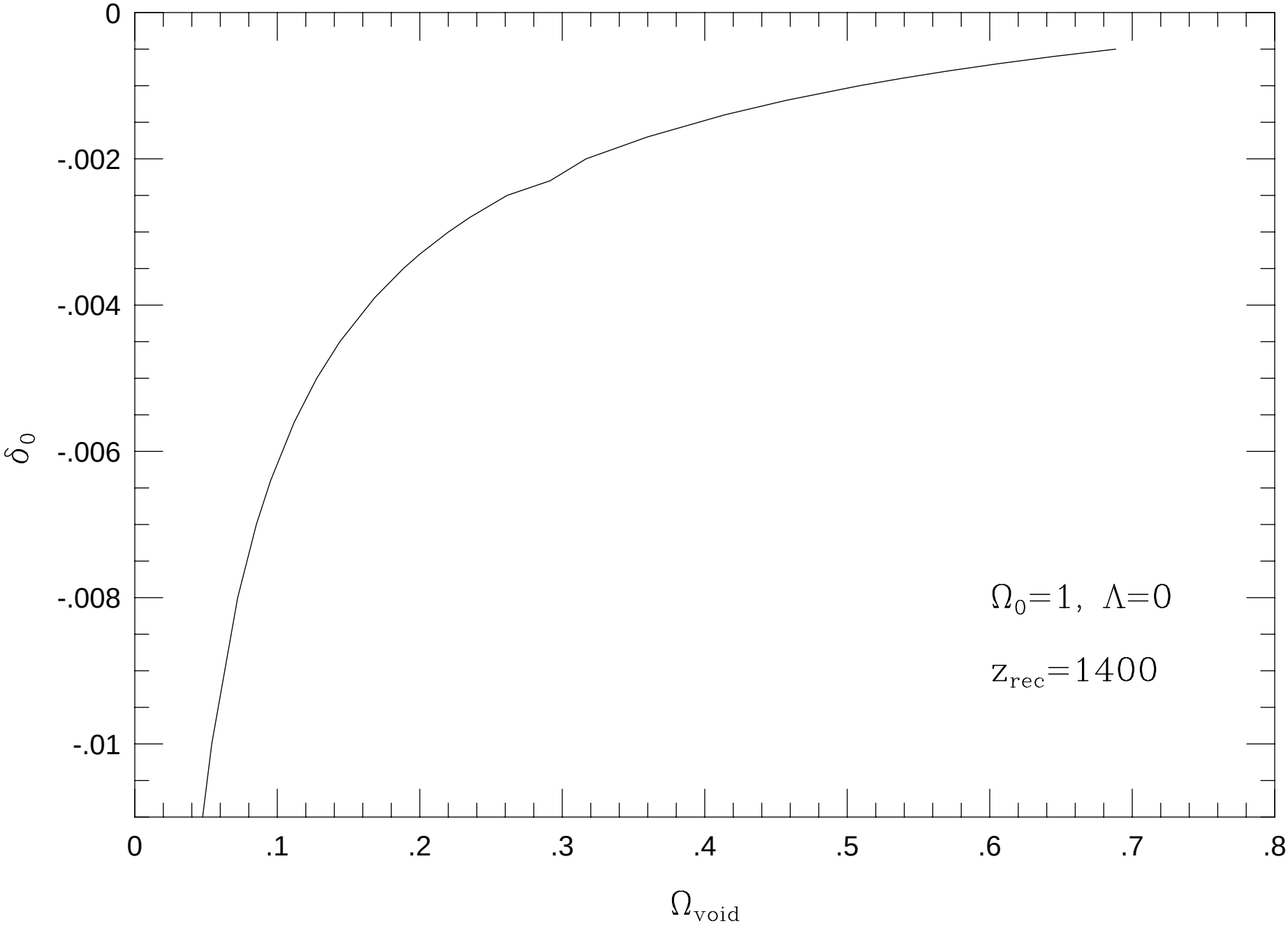
0
-.002
-.004
-.006
-.008
-.01
δ_0
0
.1
.2
.3
.4
.5
.6
.7
.8
Ω_{void}
$\Omega_0=1,\ \Lambda=0$
$z_{rec}=1400$

Figure 3

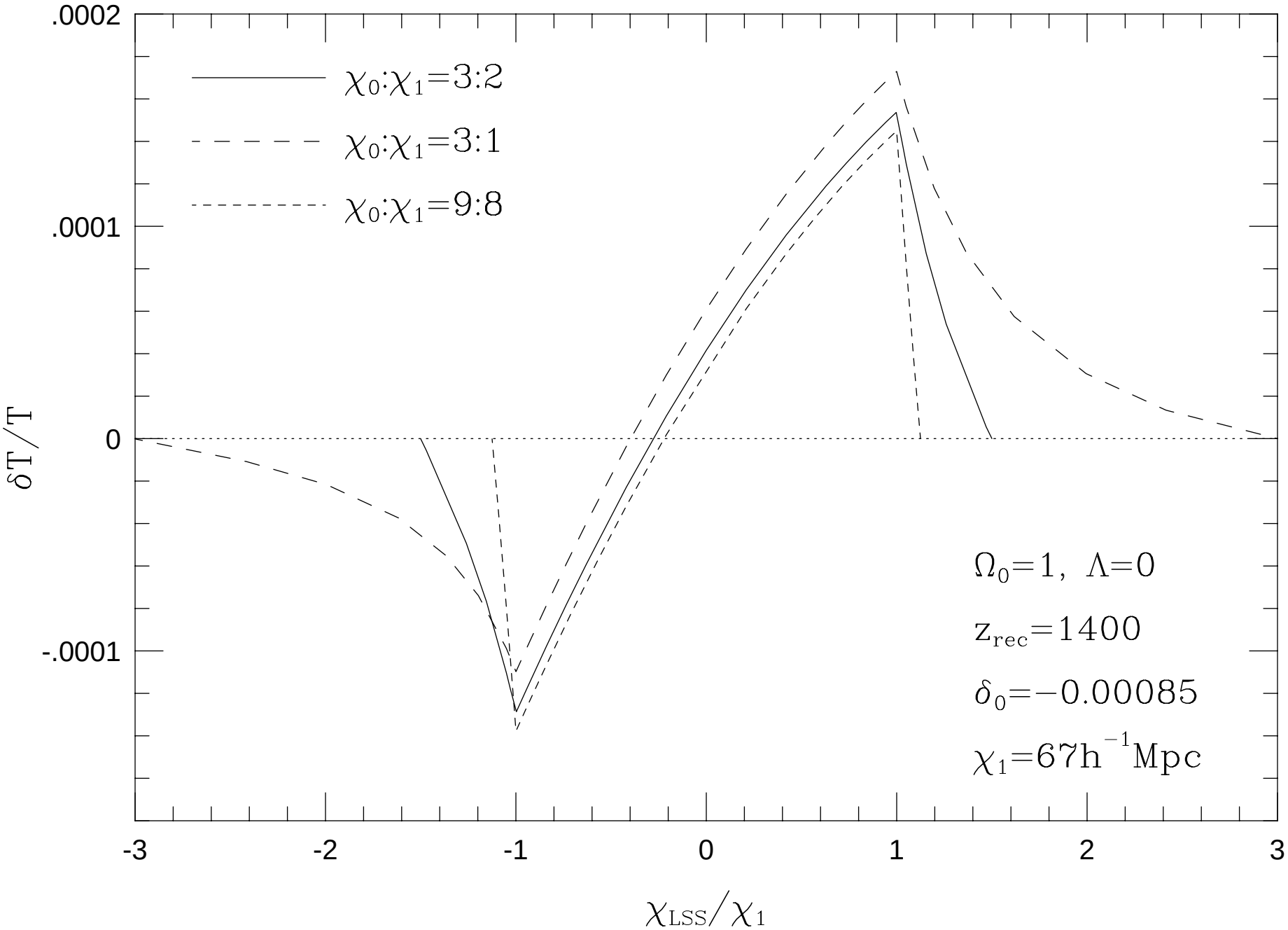
.0002
.0001
0
-.0001
δT/T
-3
-2
-1
0
1
2
3
χLSS/χ1
χ0:χ1=3:2
χ0:χ1=3:1
χ0:χ1=9:8
Ω0=1, Λ=0
zrec=1400
δ0=−0.00085
χ1=67h−1Mpc

Figure 4

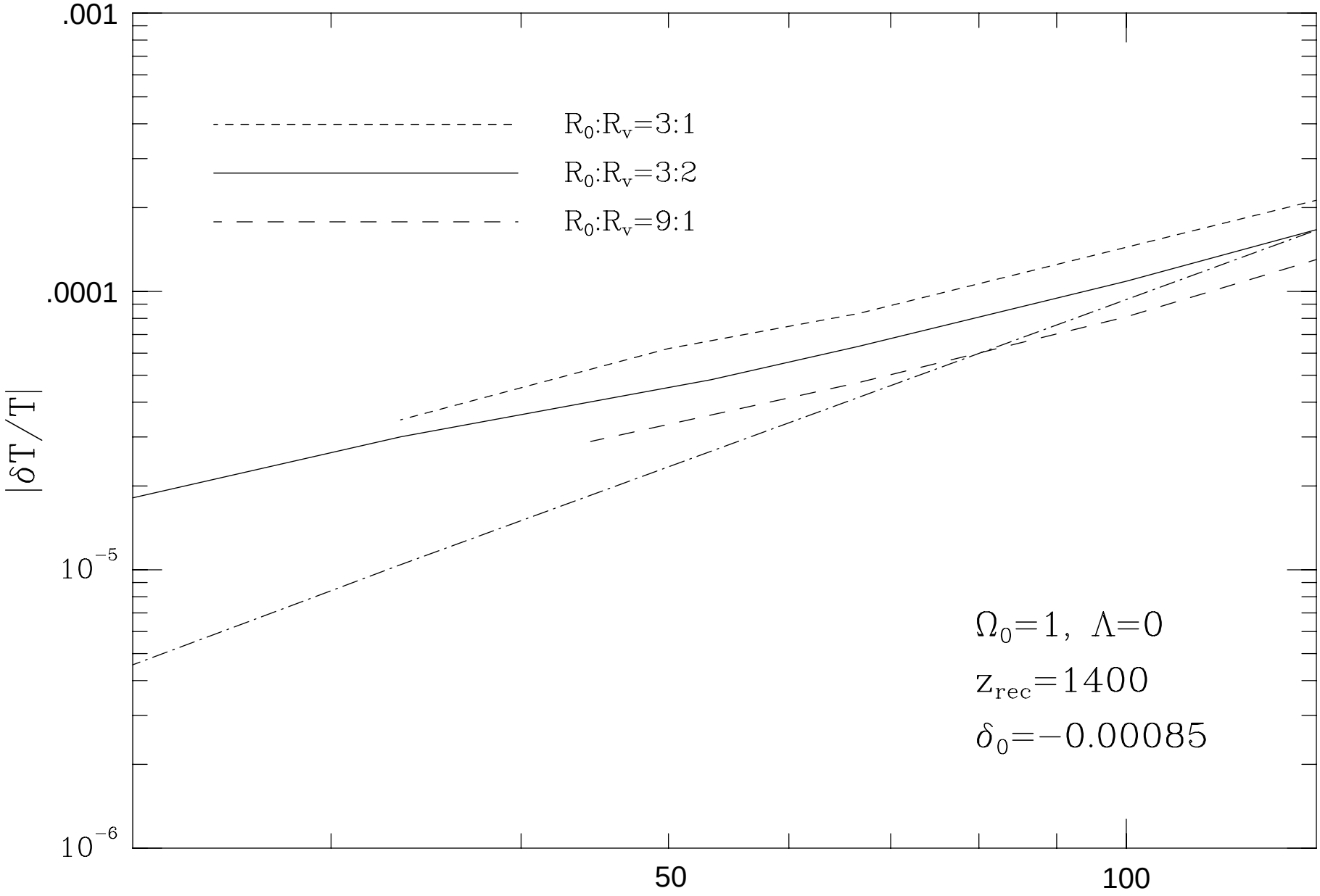
.001
.0001
10^{-5}
10^{-6}
$|\delta T/T|$
R_0:R_v=3:1
R_0:R_v=3:2
R_0:R_v=9:1
Ω_0=1, Λ=0
z_{rec}=1400
δ_0=−0.00085
50
100
$(1+z_{rec})\chi_1$ (h^{-1}Mpc)

Figure 5

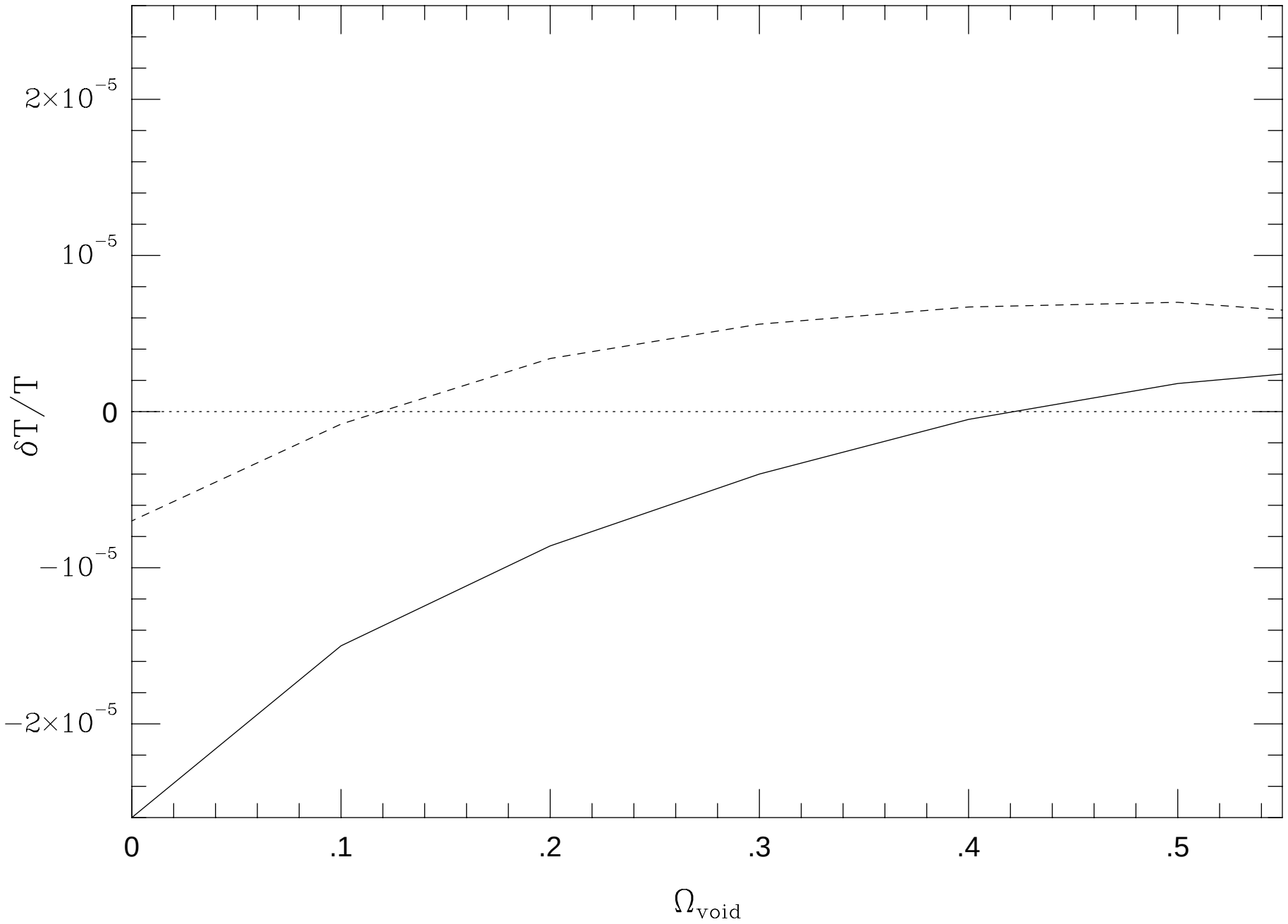

Figure 6

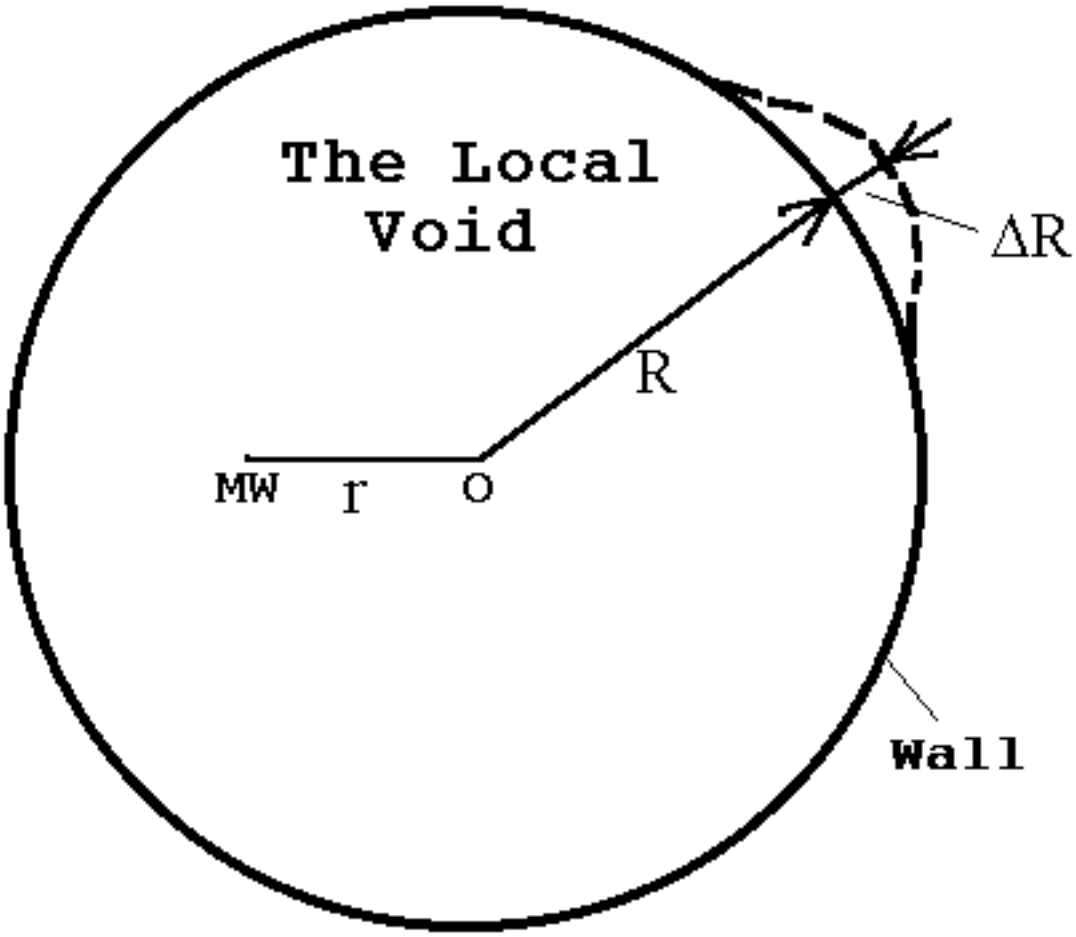

Figure 7

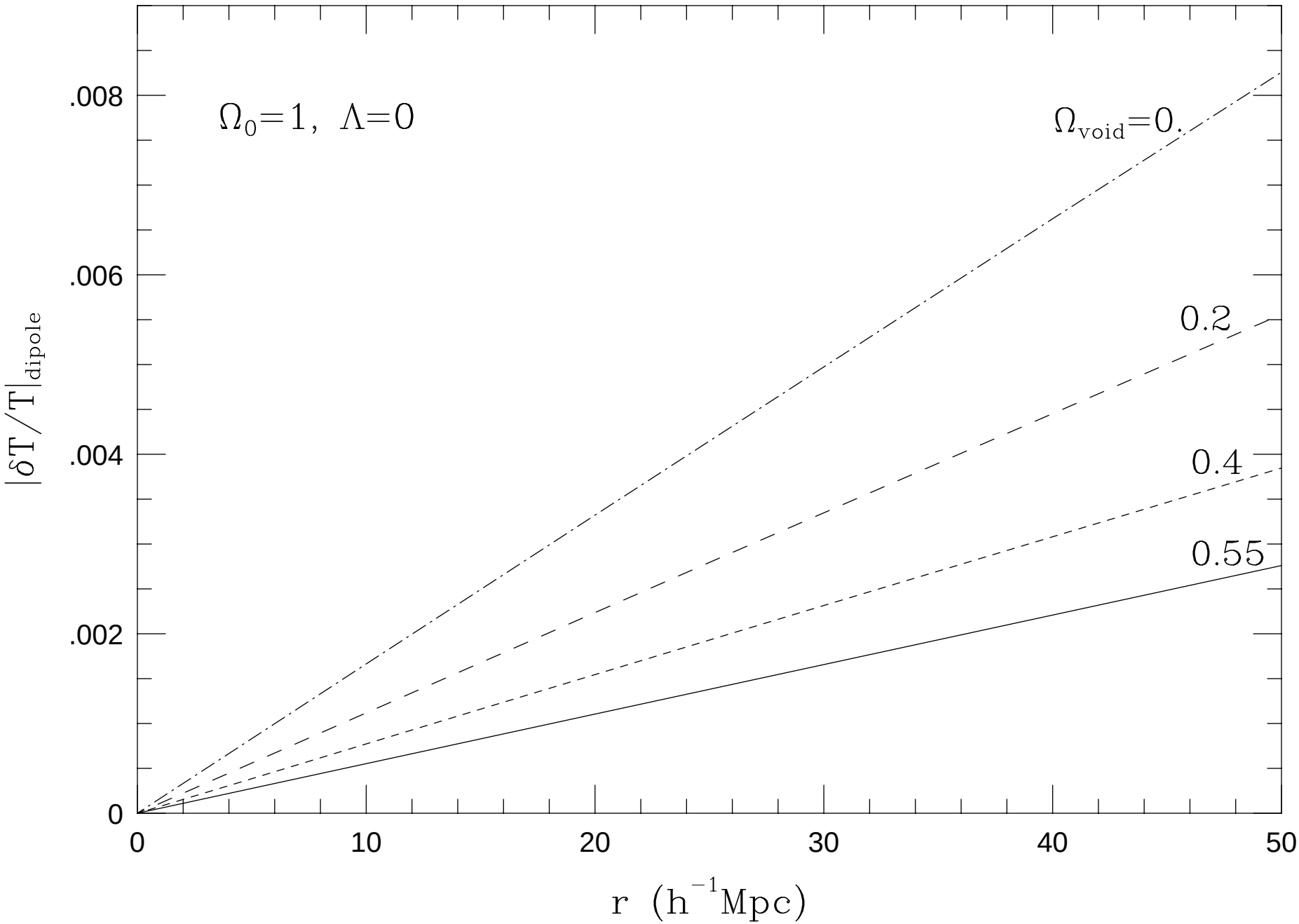
$\Omega_0=1,\ \Lambda=0$
$\Omega_{\rm void}=0.$
0.2
0.4
0.55
.008
.006
.004
.002
0
0
10
20
30
40
50
$|\delta T/T|_{\rm dipole}$
r (h^{-1}Mpc)

Figure 8